REVIEW

Check for updates

Journal of
Sensor Science and Technology

The Korean Sensors Society

# Solution-Processed van der Waals Thin Films: From Scalable Fabrication of Electronic Devices to Advanced Optoelectronic Applications

**Jihyun Kim[1] and Joohoon Kang[1,+]**

[1]*Department of Chemical and Biomolecular Engineering, Yonsei University, Seoul 03722, Republic of Korea*

**Cite This:** *J. Sens. Sci. Technol. Vol. 35, No. 1 (2026) 30-40*

https://doi.org/10.46670/JSST.2026.35.1.30

**ABSTRACT:** Solution-processed van der Waals (vdW) thin films—stacks of two-dimensional (2D) building blocks—have emerged as a scalable platform for next-generation electronic and optoelectronic applications. Recent advances in molecular intercalation exfoliation have enabled the scalable production of high-quality 2D nanosheets with large lateral size and narrow size distributions, thereby providing the essential building blocks for scalable vdW thin films. When assembled into thin films through various techniques such as spin coating, slot-die printing, inkjet printing, and photo-crosslinking, these nanosheets form conformal, ultrathin, and continuous vdW films. These structural features translate into superior electrical and optoelectrical properties, including reduced inter-sheet junction resistance, enhanced gate-to-channel electrostatic coupling, strong optoelectronic responses (e.g., high photoresponsivity). Furthermore, deliberately engineered vdW heterostructure films demonstrated advanced optoelectronic functionalities, including optical synaptic behavior and reconfigurable photodetection, paving the route for in-sensor computing. This review provides a comprehensive overview of recent progress in the scalable fabrication and device integration of solution-processed vdW thin films, highlighting their potential for large-area, high-performance electronic and optoelectronic systems.

**KEYWORDS:** *van der Waals thin film, Solution-based processing, Electronics, Optoelectronics*

## 1. INTRODUCTION

Two-dimensional (2D) materials have garnered significant attention due to their unique physical, electronic, and optoelectronic properties [1-6]. Among these, van der Waals (vdW) thin films—composed of stacked 2D layers—have emerged as highly promising candidates for next-generation device technologies [7-15]. The artificially engineered interfaces within vdW thin films enable exotic phenomena such as band modulation [16], promoted charge transport [17], and exciton-assisted tunneling [18], which cannot be realized in individual 2D materials. These interfacial effects are particularly advantageous for achieving high-performance electronic and optoelectronic platforms. For example, a representative vdW heterostructure device comprising molybdenum disulfide ($MoS_2$)/hexagonal boron nitride (h-BN)/graphene demonstrates precise gate-controlled switching between high- and low-resistance states and efficient carrier transport, while simultaneously exhibiting extraordinary optoelectronic performance with a photoresponsivity of $4.4 \times 10^6$ A $W^{-1}$ and a detectivity of $1.4 \times 10^{17}$ Jones [19]. These outstanding metrics, arising from deliberately designed interfacial junctions at the heterogeneous vdW interfaces, underscore the vast potential of vdW thin films for advanced electronic and optoelectronic applications.

Despite these advances, the practical potential of vdW thin films remains constrained by the complexity of their fabrication. Conventional approaches typically rely on micromechanical exfoliation of bulk crystals combined with microscope-assisted stacking and alignment. While these techniques have been instrumental in fundamental studies, they are inherently labor-intensive, low-throughput, and unsuitable for large-scale integration. This has driven the exploration of alternative processing as a scalable and cost-effective route for producing high-quality vdW thin films.

To address these challenges, solution-based processing has

[+]Corresponding author: joohoon@yonsei.ac.kr
Received : Dec. 11, 2025, Accepted : Dec. 19, 2025

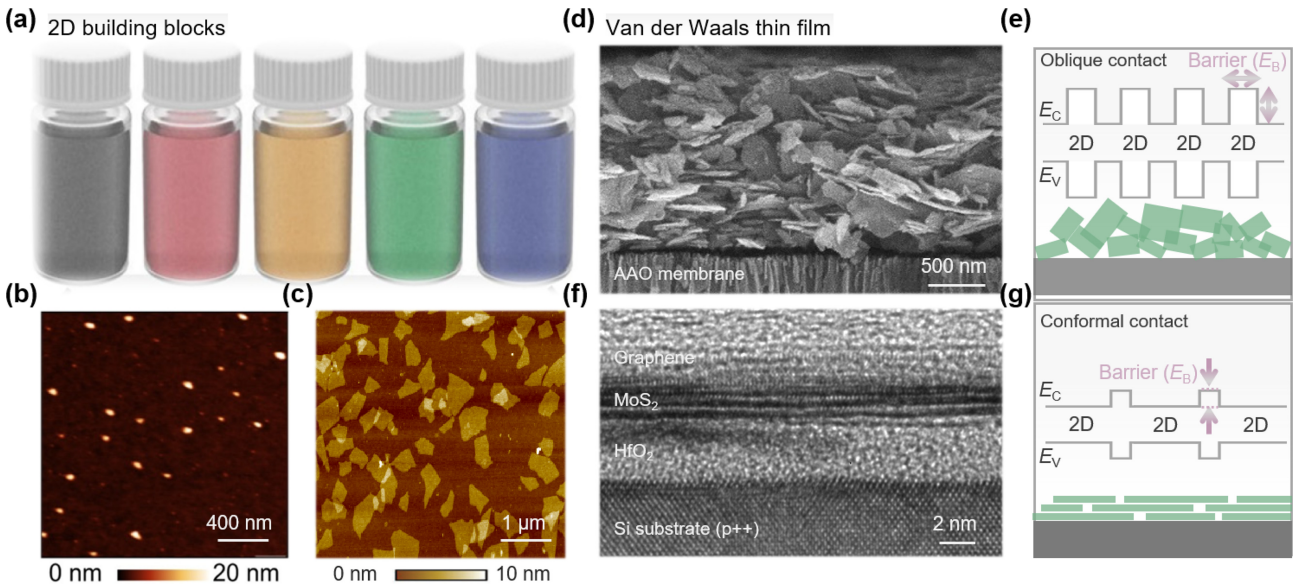


**Fig. 1.** 2D building blocks and vdW thin film structures. (a) Schematic illustration of solution-processed dispersions of various 2D materials. (b, c) AFM images of nanosheets obtained from LPE (b), showing small lateral sizes (<100 nm) and from MIE (c), exhibiting large lateral sizes (>1 μm) with narrow thickness distribution. Adapted from Ref. [31]. (d) Cross-sectional SEM image of a LPE-derived vdW thin film assembled on an anodic aluminum oxide membrane. Adapted from Ref. [25]. (e) Schematic illustration of LPE-based vdW thin film, where oblique inter-sheet contacts introduce significant junction barriers. (f) High-resolution TEM image of a MIE-based vdW thin film comprising graphene/$MoS_2$/$HfO_2$. Adapted from Ref. [36]. (g) Schematic illustration of MIE-based vdW thin film, showing conformal contacts with reduced junction barriers.

emerged as a promising alternative for producing and assembling 2D building blocks into vdW thin films [20-24]. Leveraging their intrinsic scalability, solution-based approaches enable uniform film formation over large areas, offering a route toward industrial-scale manufacturing. Among these, liquid-phase exfoliation (LPE), which utilizes ultrasonication to apply mechanical energy and exfoliate bulk crystals into 2D materials, has been widely employed to prepare materials such as $MoS_2$ [25,26], black phosphorus (BP) [27,28], and indium selenide (InSe) [29] for scalable device fabrication. However, the intense mechanical forces applied during the LPE process often produce nanosheets with small lateral sizes and broad size distributions, which can compromise the structural features (e.g., packing order and density) of the resulting films [20]. Consequently, LPE-derived vdW thin films exhibit oblique inter-sheet contacts, leading to high inter-sheet resistance and, in turn, limited electronic and optoelectronic performance [30].

To overcome these issues, molecular intercalation-based exfoliation (MIE) has been developed. This method introduces bulky organic cations or other molecular species between the layers of bulk crystals, expanding the interlayer spacing and thereby enabling the exfoliation process even under lower mechanical energy [31,32]. As a result, this approach yields 2D nanosheets with larger lateral sizes, narrower size distributions, and reduced thicknesses compared to those obtained via conventional LPE. When these high-quality nanosheets are assembled into vdW thin films, they form more conformal inter-sheet contacts and highly packed structures, which significantly reduce junction resistance and enhance charge transport efficiency [30]. These improvements directly translate into superior electrical and optoelectrical characteristics such as high carrier mobility and photoresponsivity in device applications.

In this work, we review recent advancements in solution-processed vdW thin films and their integration into electronic and optoelectronic devices. We first examine the fundamental characteristics of vdW thin films assembled from 2D building blocks prepared via LPE and MIE, emphasizing how the differences in nanosheet size and thickness critically affect the structural characteristics of the resulting films. We then explore scalable assembly techniques—including spin coating, slot-die coating, inkjet printing, and photo-crosslinking—that enable the production of uniform and large-area vdW thin films with controlled structural features. Building upon these fabrication and structural insights, we further discuss their electrical and optoelectronic characteristics, highlighting demonstrations of high carrier mobility, low-voltage operation, and enhanced photoresponsivity, as well as advanced functionalities such as optical synaptic behavior and reconfigurable photodetection.

## 2. 2D BUILDING BLOCKS AND vdW THIN FILM STRUCTURES

For scalable vdW thin film formation, a variety of 2D materials have been developed in the form of stable dispersions, including semiconductors ($MoS_2$, BP, InSe), metallic conductors (graphene, MXene), and insulators ($HfO_{2-x}$, $ZrO_{2-x}$) (Fig. 1(a)). This diversity of 2D materials demonstrates their applicability as various functional components in electronic and optoelectronic devices. For such applications, the structural properties of the nanosheets are crucial, as they directly impact charge transport within vdW thin films. Importantly, these characteristics vary significantly with the synthesis route, particularly between LPE and MIE. LPE typically relies on strong mechanical energy input, such as ultrasonication, to overcome interlayer vdW forces. This process produces nanosheets with small lateral dimensions (<100 nm) and broad size distributions (Fig. 1(b)). In contrast, MIE introduces molecular species (e.g., large organic cations) between the crystal layers, weakening interlayer interactions and allowing exfoliation under milder mechanical agitation. As a result, MIE yields nanosheets with large lateral sizes (>1 μm), narrow size distributions, and high aspect ratios (Fig. 1(c)). These differences in exfoliation mechanism and mechanical energy application directly influence the morphology of the resulting vdW thin films.

When assembled into vdW thin films, the contrast becomes even more pronounced. LPE-derived nanosheets, due to their small lateral size and substantial thickness, typically form relatively thick layers (>500 nm) with edge-to-edge interflake contacts (Fig. 1(d)) [25]. Such oblique contacts increase junction resistance and introduce substantial transport barriers ($E_B$) between adjacent nanosheets (Fig. 1(e)). Moreover, the resulting film thickness weakens electrostatic modulation across the channel, further limiting device performance. By contrast, vdW thin films derived from MIE nanosheets exhibit ultrathin, densely packed morphologies with conformal plane-to-plane contacts (Fig. 1(f)). These interfaces resemble natural vdW stacking in bulk layered crystals, leading to reduced junction resistance, lowered $E_B$, and significantly improved charge transport efficiency (Fig. 1(g)). Notably, these advantageous structural characteristics can be preserved even after heterogeneous integration of multiple vdW thin films (see the graphene/$MoS_2$ stack in Fig. 1(f)) [33], opening opportunities for diverse material designs and device architectures. Building upon this foundation, the following sections discuss scalable production strategies for MIE-derived building blocks and examine how their structural, electrical, and optoelectronic properties can be harnessed for electronic and optoelectronic device applications.

## 3. STRATEGIES FOR FABRICATING vdW THIN FILMS

Building on the structural advantages of high-quality nanosheets prepared via MIE, the next crucial step toward practical device integration is the scalable assembly of these 2D building blocks into continuous vdW thin films. To achieve this, a variety of solution-based assembly techniques have been developed, offering large-area coverage, high spatial uniformity, and compatibility with industrial manufacturing. These approaches not only enable uniform thin film deposition but also provide versatile patterning capabilities, which are essential for fabricating electronic and optoelectronic device arrays.

Spin coating is one of the most straightforward and widely used methods for depositing 2D building blocks. For example, sequential spin-coating $MoS_2$ ink onto a $SiO_2$ wafer yields a highly uniform film, as evidenced by the consistent greenish film observed across the entire substrate (Fig. 2(a), left). This uniformity arises from the preferential in-plane alignment of high-aspect-ratio nanosheets parallel to the wafer surface (Fig. 2(a), right), which minimizes inter-sheet voids and enhances film continuity [34].

Additionally, to bridge the gap between laboratory-scale demonstrations and industrial-scale production, slot-die printing has been adopted (Fig. 2(b)). By optimizing process parameters, this method can deposit vdW thin films over wafer-scale substrates (e.g., 5-inch) within several seconds [35]. Furthermore, the sequential deposition of multiple functional layers—such as vdW channels and oxide dielectrics—has enabled the realization of heterogeneous films for wafer-scale transistor arrays. A notable advantage of slot-die printing is its facile thickness tunability, a parameter that critically influences device performance and can be precisely controlled by adjusting the ink concentration (Fig. 2(c)).

For scalable device fabrication, precise and efficient patterning of vdW thin films is equally essential. Inkjet printing has emerged as a versatile method for this purpose, as this approach enables the formation of customizable patterns without using photolithography [36-38]. Its applicability has been demonstrated using various 2D material inks, including graphene, $MoS_2$, and $HfS_2$ [36]. For example, stable ejection of $MoS_2$ ink results in the generation of single droplets without undesirable satellite droplets—an essential requirement for reliable operation (Fig. 2(d), upper). Repeated deposition subsequently yields periodic dot arrays with high spatial uniformity, as confirmed by photoluminescence (PL) mapping (Fig. 2(d), lower).

Recently, photo-crosslinking has been introduced as an

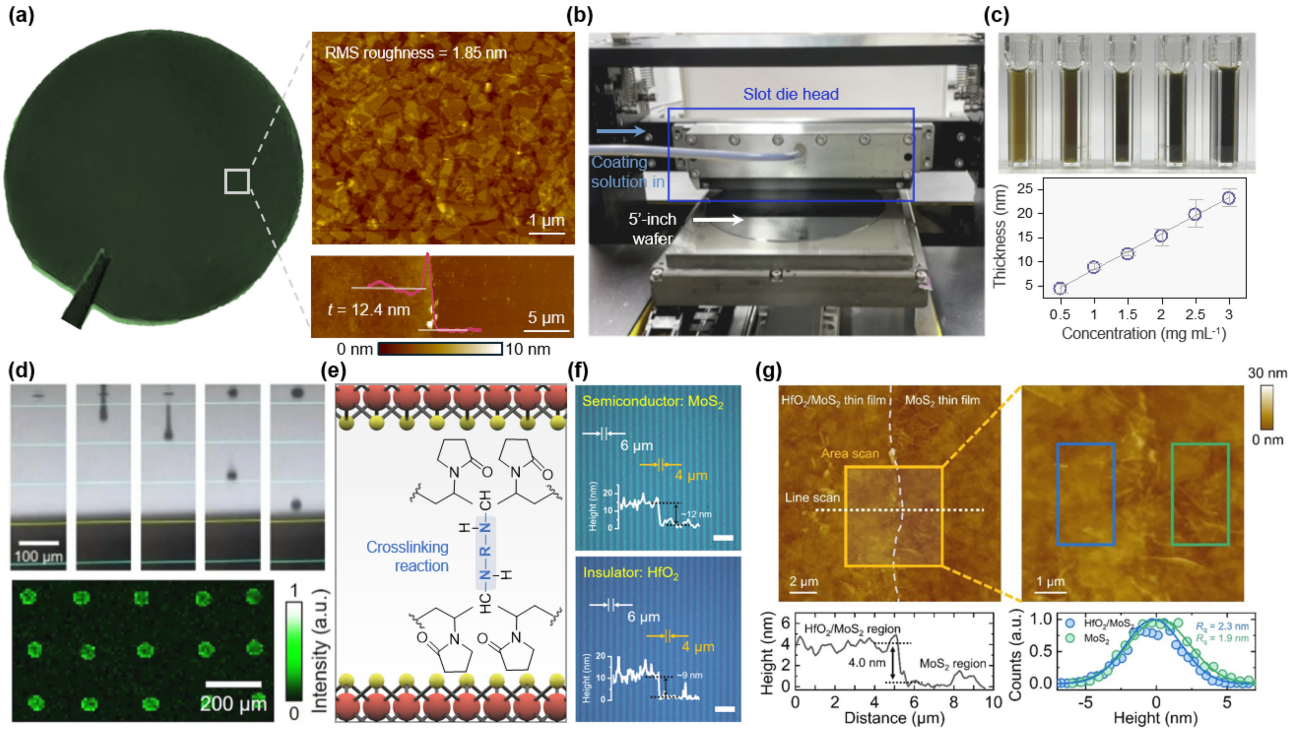


**Fig. 2.** Strategies for fabricating vdW thin films. (a) Uniform $MoS_2$ thin film deposited by multiple spin coating on a 2-inch $SiO_2$/Si wafer (left), with AFM images showing in-plane alignment of nanosheets (top right) and corresponding thickness profile (bottom right). Adapted from Ref. [34]. (b) Slot-die printing setup for large-area vdW thin film fabrication, enabling rapid deposition on a 5-inch wafer. (c) Photographs of $MoS_2$ inks at various concentrations (top) and resulting film thickness as a function of ink concentration (bottom), demonstrating controllable thickness tuning. Adapted from Ref. [35]. (d) Optical microscopy images of inkjet-printed $MoS_2$ droplets (top) and PL mapping of printed dot arrays (bottom). Adapted from Ref. [36]. (e) Schematic of photo-crosslinking between phenyl azide groups and residual PVP chains on nanosheets under UV irradiation. (f) Optical microscopy and AFM profiles of patterned $MoS_2$ films (top) and $HfO_2$ films (bottom) with resolutions down to 4 μm. (g) AFM images and corresponding height analysis of $HfO_2$/$MoS_2$ and $MoS_2$ regions, confirming minimal surface residues and contamination-free, conformal interfaces. Adapted from Ref. [39].

alternative strategy to achieve both high-resolution patterning and chemically clean interfaces [39,40]. In this method, photoactive crosslinkers—such as phenyl azide molecules—are incorporated into the coated vdW thin films. Upon UV irradiation, crosslinking occurs between the crosslinker and the polyvinylpyrrolidone (PVP) surfactant remaining in the film, enhancing the mechanical robustness of the selected regions (Fig. 2(e)). Subsequent sonication removes the uncrosslinked areas, leaving only the patterned vdW film. Through this approach, various types of vdW thin films (e.g., $MoS_2$ and graphene) have been successfully patterned, while achieving resolutions down to ~4 μm without the use of photoresist, developer, or other organic chemicals typically required for photolithography (Fig. 2(f)). Moreover, owing to the contamination-free nature of this method, conformal and clean interfaces are preserved even during heterogeneous integration, as verified in Fig. 2(g), and these interfaces are crucial for high-performance device operation.

## 4. ELECTRICAL CHARACTERISTICS OF vdW THIN FILMS

Building on the scalable fabrication strategies described in the previous section, the charge transport behavior within vdW thin films plays a pivotal role in determining their potential for electronic and optoelectronic applications. Once uniform films are formed through deposition techniques, factors such as interfacial cleanness, film morphology, and nanosheet packing directly influence transport behavior within vdW thin films. Therefore, a clear understanding of the relationship between material characteristics and electrical properties is essential for the successful implementation of these films in device applications.

An early report on $MoS_2$ vdW thin film devices arrays demonstrated the feasibility of scalable electronics, achieving high device performance with narrow device-to-device variations [32]. Subsequent research has focused on further performance enhancement through strategies such as

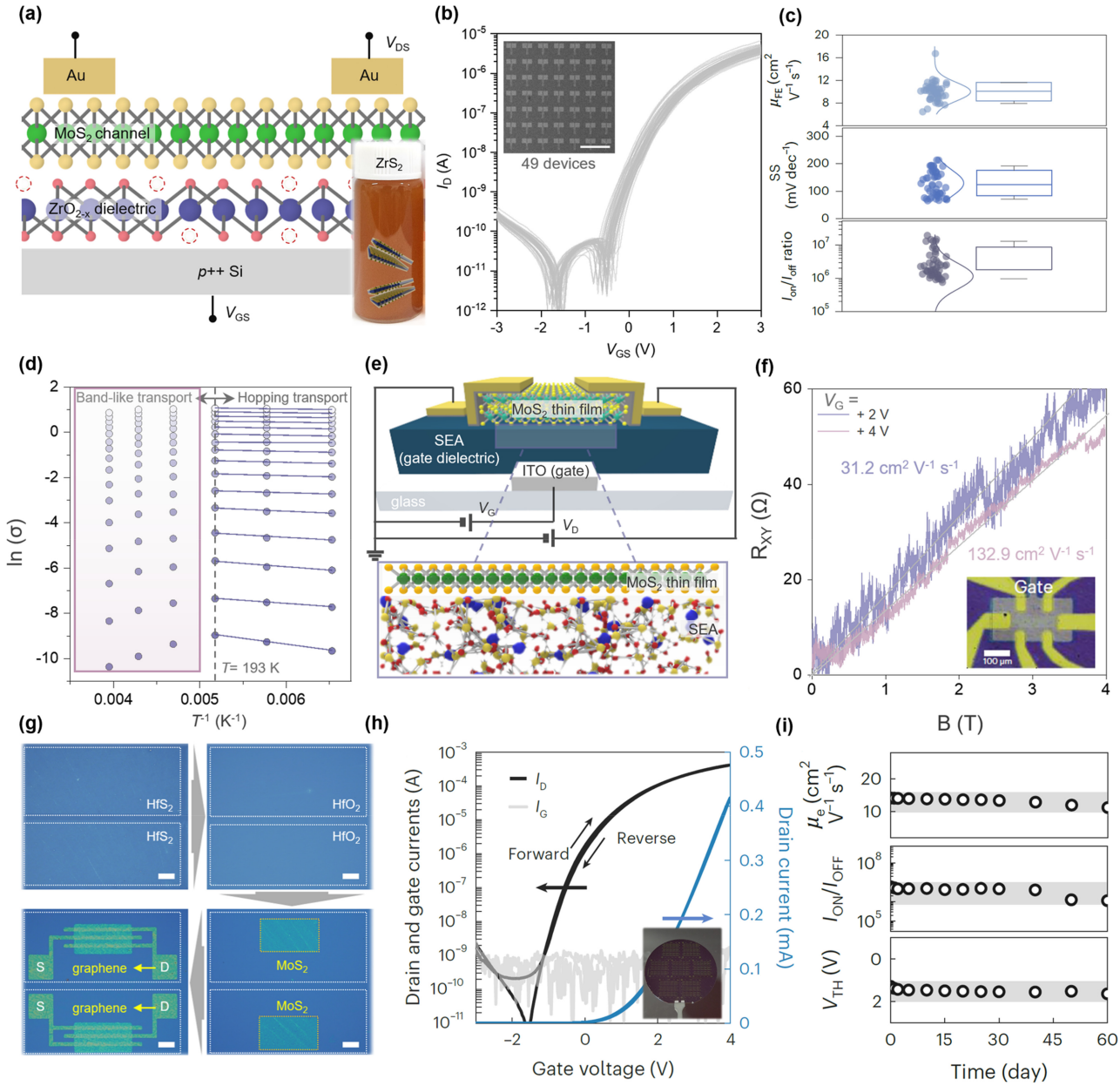


**Fig. 3.** Electrical characteristics of vdW thin films. (a) Schematic illustration of a heterogeneous $MoS_2/ZrO_{2-x}$ transistor structure prepared by coating $ZrS_2$ ink on $p^{++}$ Si, oxidizing to $ZrO_{2-x}$, and stacking $MoS_2$ thin film. (b) Representative transfer curves of 49 devices showing uniform n-type behavior at low operating voltages; inset: optical micrograph of the device array. (c) Statistical distributions of $\mu_{FE}$, SS, and $I_{on}/I_{off}$. (d) Temperature-dependent conductivity plots revealing band-like transport characteristics. Adapted from Ref. [41]. (e) Schematic of a sequentially printed SEA gate dielectric/$MoS_2$ channel transistor. (f) Hall measurements confirming high carrier mobility of 31.2 and 132.9 $cm^2$ $V^{-1}$ $s^{-1}$ for $V_{GS}$ = 2 and 4 V, respectively); inset: optical image of the Hall bar device. Adapted from Ref. [35]. (g) Optical images of patterned $HfS_2$, $HfO_2$, graphene, and $MoS_2$ thin films fabricated via photo-crosslinking. (h) Transfer characteristics of photo-crosslinked vdW thin film transistor; inset: photographic image of transistor arrays. (i) Long-term stability of $\mu_{FE}$, $I_{on}/I_{off}$, and $V_{TH}$ over 60 days. Adapted from Ref. [39].

heterogeneous integration. One strategy incorporates $ZrO_{2-x}$ vdW thin film as a gate dielectric with $MoS_2$ film as the semiconducting channel (Fig. 3(a)) [41]. The resulting transistor arrays exhibit n-type transport at low operating voltages, enabled by the high capacitance of $ZrO_{2-x}$ (Fig. 3(b)). Conformal interfaces preserved during integration ensure highly uniform charge transport, as confirmed by statistical analysis of 49 devices: an average field-effect mobility ($\mu_{FE}$) of 10 $cm^2$ $V^{-1}s^{-1}$, subthreshold swing (SS) of 129 mV $dec^{-1}$, and an on/off current ratio ($I_{on}/I_{off}$) of ~2 × $10^6$, all with minimal

distribution (Fig. 3(c)). These metrics are comparable to those of other large-area 2D devices fabricated by chemical vapor deposition (CVD) [42-46]. Notably, the devices also exhibit highly efficient charge transport, band-like charge transport—typically observed only in high-quality 2D systems—highlighting the potential of heterogeneous vdW thin film for high-performance electronic applications (Fig. 3(d)).

Another strategy to boost charge transport performance involves the sequential printing of sodium-embedded alumina (SEA) and $MoS_2$ thin films (Fig. 3(e)) [35]. The printed SEA dielectric, characterized by high capacitance due to mobile sodium ions, forms flat and uniform interface with the $MoS_2$ thin film, effectively suppressing charge scattering. As a result, this configuration achieves an impressive average $\mu_{FE}$ of 80 $cm^2\ V^{-1}s^{-1}$, with Hall measurements confirming a mobility as high as 133 $cm^2\ V^{-1}s^{-1}$ (Fig. 3(f)).

Beyond material integration, advancements in patterning processes have also played a crucial role in improving device performance and simplifying fabrication. Photo-crosslinking technique, for instance, enables the sequential stacking of multiple vdW thin film layers without damaging underlying layers [39]. By eliminating conventional photolithography and etching processes, this method minimizes contamination and preserves pristine interfaces. For example, $HfO_2$, $MoS_2$, and graphene thin films have been patterned in sequence to serve as the gate dielectric, semiconducting channel, and electrodes, respectively (Fig. 3(g)). Devices fabricated using this approach exhibit n-type transport at low operating voltages and show negligible hysteresis (~40 meV), comparable to mechanically exfoliated $MoS_2$ devices. Furthermore, the devices exhibit long-term operational stability, clearly demonstrating the practical applicability of such vdW thin film devices in reliable, large-scale electronic systems (Fig. 3(i)).

## 5. OPTOELECTRICAL FEATURES OF vdW THIN FILM DEVICES

The optimized electrical characteristics of solution-processed vdW thin films, as discussed in the preceding sections, provide a robust foundation for advancing their optoelectronic functionalities. Owing to their material diversity, solution-processed vdW thin films have demonstrated a wide range of photodetection capabilities—from broadband detection with high responsivity to optical synaptic behaviors suitable for in-sensor computing.

A representative demonstration involves heterogeneous vdW thin film devices integrating $HfO_2$, $MoS_2$, and graphene, which exhibit broadband photodetection with gate-tunable performance (Fig. 4(a)-(b)) [33]. In this device architecture, the $MoS_2$ thin film serves as a photoactive channel, efficiently absorbing photons across the visible spectrum (450–655 nm), while the high-capacitance $HfO_2$ film enables photodetection even under low gate biases. This synergistic configuration yields exceptional photoresponsivity, reaching approximately $10^5$ A $W^{-1}$ at $V_{GS}$ = 1 V (Fig. 4(c)), surpassing the performance of most large-area 2D photodetectors. Such outstanding performance is attributed to the unique structural attributes of solution-processed vdW thin films: the high fraction of monolayer building blocks ensures strong quantum efficiency, while the stacked nature of the film enhances optical absorption. These results highlight the intrinsic advantages of vdW thin films for high-performance photodetection, underscoring their potential for realizing scalable, next-generation optoelectronic devices.

Beyond $MoS_2$-based devices, the compositional flexibility of vdW thin films enables spectral tunability across diverse wavelength regimes. For example, BP nanosheets, with their narrow bandgap, have been assembled into vdW thin films (Fig. 4(d)), enabling photodetection in the near-infrared (NIR) regime up to 1550 nm (Fig. 4(e)) [47]. These devices exhibit stable photocurrent responses under consecutive NIR illumination, with rapid rise and decay times (5.1 ms and 6.8 ms, respectively), which are highly desirable for optical communication technologies. In parallel, semiconducting MXene thin films have demonstrated broadband detection across the visible spectrum (Fig. 4(f)), benefiting from their wide optical absorption window [48]. Collectively, these studies highlight the compositional tunability of solution-processed vdW thin films and their capability to meet application-specific spectral demands [49].

In addition to broadband detection capabilities, solution-processed vdW thin films exhibit emerging functionalities relevant to neuromorphic and in-sensor computing. These capabilities are primarily enabled by defect-induced electronic states within the thin film (Fig. 4(g)). For example, $MoS_2$ thin films demonstrate optically induced conductance modulation with retention, driven by defect-mediated carrier trapping [50]. This phenomenon leads to optical synaptic-like behavior, where device conductance is gradually potentiated under repeated light pulses and returns to its baseline state upon removal of the optical stimulus (Fig. 4(h)). This behavior extends the role of vdW thin films beyond conventional photodetection, enabling their use in in-sensor computing applications. Notably, device arrays based on vdW thin films have demonstrated the ability to preprocess optical images by enhancing spatial sharpness when illuminated with patterned light sources (Fig. 4(i)).

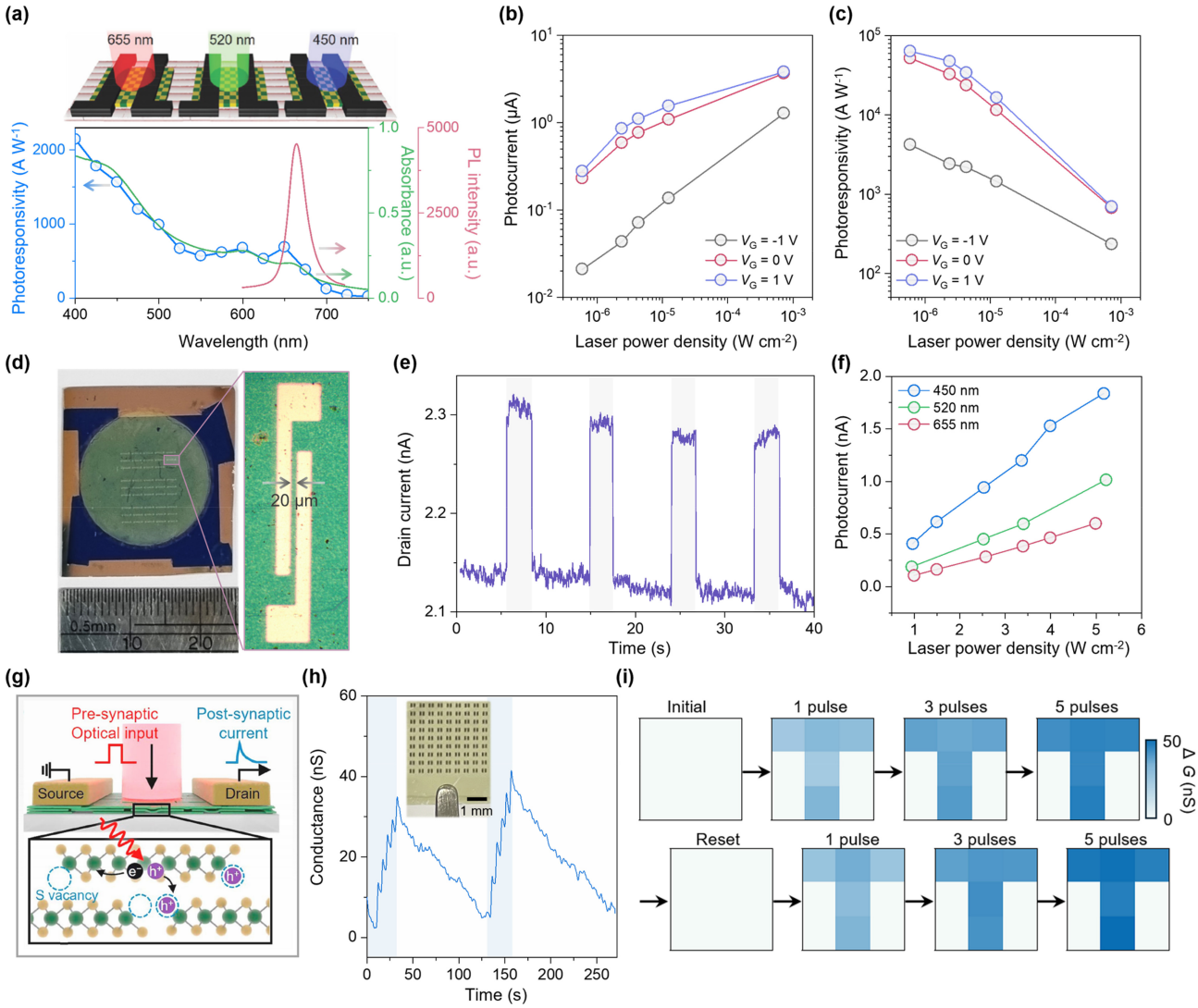


**Fig. 4.** Optoelectrical features of vdW thin film devices. (a) Spectral photoresponsivity along with an absorbance and PL spectrum obtained from $HfO_2/MoS_2$/graphene heterogeneous thin film devices. (b) Photocurrent and (c) photoresponsivity as a function of laser power density at various gate biases. Adapted from Ref. [33]. (d) Optical image of large-area BP thin film device arrays fabricated on a wafer, with a magnified view of an individual channel. (e) Time-resolved photocurrent response of BP thin film under 1550 nm periodic light on/off switching. Adapted from Ref. [47]. (f) Photocurrent of MXene thin film devices as a function of laser power density under illumination at different wavelengths (450, 520, and 655 nm). Adapted from Ref. [48]. (g) Schematic illustration of optically induced synaptic behavior in defect-mediated $MoS_2$ vdW thin films. (h) Conductance modulation of $MoS_2$ thin film under repeated optical stimulation. (i) Optical pulse-dependent synaptic weight changes, showing potentiation and reset characteristics. Adapted from Ref. [50].

## 6. ADVANCED OPTOELECTRONIC OPERATION OF vdW THIN FILM DEVICES

Recent developments in vdW thin film devices have demonstrated that these films not only have potential for conventional optoelectronic applications but also enable advanced functionalities such as reconfigurable operation. This ability to dynamically switch between distinct optoelectrical features within a single device configuration is particularly crucial for next-generation optoelectronic systems that require adaptability.

A representative example is the integration of $MoS_2$ thin film with sub-stoichiometric $ZrO_{2-x}$ thin film, where intrinsic oxygen vacancies in $ZrO_{2-x}$ play a pivotal role in governing photoexcited carrier dynamics (e.g., fast and slow decay times) [41]. To exploit this, two distinct operation modes—conventional global gating and uniquely designed local gating—are employed to control photoexcited carrier dynamics. As illustrated in Fig. 5(a), two distinct operation modes can be defined depending on the applied bias

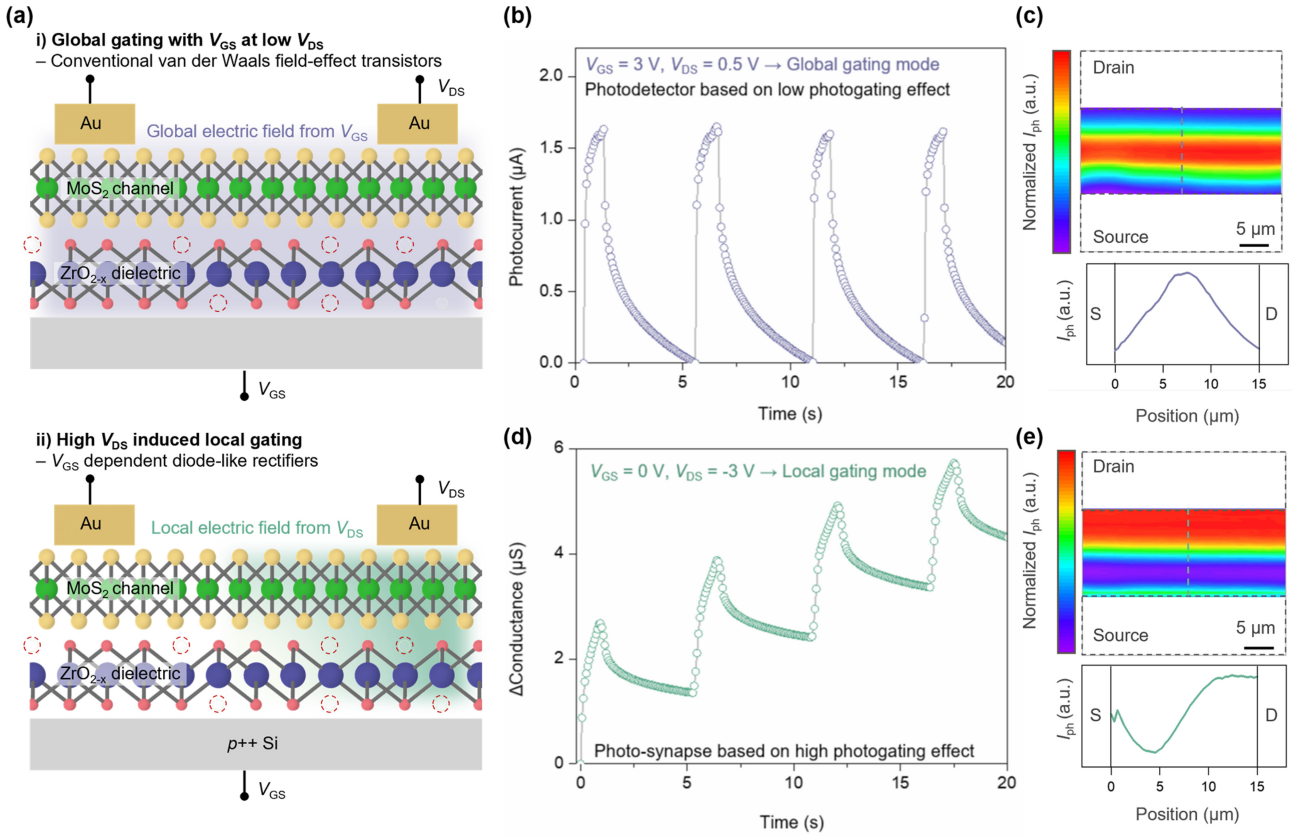


**Fig. 5.** Advanced optoelectronic operation of vdW thin film devices. (a) Schematic illustrations of operation mechanisms: (i) global gating mode, where a uniform electric field across the device results in conventional phototransistor behavior, and (ii) local gating mode, where a drain-induced vertical electric field activates photosynaptic behavior. (b) Temporal photocurrent response under global gating mode, showing fast decay characteristic. (c) Spatial photocurrent mapping under global gating mode, revealing Gaussian-like distribution. (d) Conductance modulation under repeated light pulses in local gating mode, showing photosynaptic behavior. (e) Spatial photocurrent mapping under the local gating mode, showing a non-uniform distribution with photocurrent predominantly localized near the drain region. Adapted from Ref. [41].

configuration. Under global gating conditions ($V_{GS} >> V_{DS}$), the electric field is uniformly distributed across the $MoS_2$ film, and the device operates as a conventional phototransistor (upper panel of Fig. 5(a)). In this mode, photocurrent is generated and only trapped in only a few shallow trap states within $MoS_2$ thin film, leading to rapid photoswitching behavior with short decay times (Fig. 5(b)). Spatial photocurrent mapping under global gating further confirms this uniform response, with photocurrent predominantly localized near the channel center and exhibiting a Gaussian distribution (Fig. 5(c)). Such characteristics are suitable for photodetector applications where rapid on/off response is required.

In contrast, as a large drain bias is applied with $V_{GS} << V_{DS}$ (local gating mode), a strong vertical electric field emerges near the drain terminal (bottom panel of Fig. 5(a)). This locally enhanced field facilitates trap-assisted tunneling of photoexcited carriers through oxygen vacancy sites in the $ZrO_{2-x}$ dielectric to back-gate electrode. Importantly, the tunneling processes lead to an enhanced photogating effect and prolonged carrier lifetimes, giving rise to slow decay dynamics and conductance accumulation under repeated light pulses (Fig. 5(d)). This behavior effectively emulates photo-synaptic responses, where conductance changes are accumulated under external optical stimuli, providing a foundation for in-sensor computing functionalities. Spatial photocurrent mapping under local gating conditions reveals non-uniform photocurrent distributions across the channel (Fig. 5(e)), consistent with the localized enhancement of the photogating effect near the drain terminal.

This dual-mode operation highlights the exceptional tunability of the optoelectronic properties in $MoS_2/ZrO_{2-x}$ heterogeneous vdW thin films. By simply adjusting the applied bias, a single device can seamlessly transition between two operational modes: (i) a high-speed photodetector optimized for conventional optoelectronic sensing, and (ii) a retentive photosynapse capable of adaptive information processing. This bias-dependent reconfigurability not only broadens the functional versatility of vdW thin film devices but also

establishes a scalable pathway toward next-generation optoelectronic platforms that integrate rapid sensing with in-sensor device functionalities.

## 7. CONCLUSION AND OUTLOOK

In summary, solution-processed vdW thin films have emerged as a highly promising platform for next-generation electronic and optoelectronic devices. By leveraging scalable exfoliation strategies such as MIE, recent research has been able to prepare high-quality 2D building blocks and assemble them into vdW thin films. Scalable deposition and patterning techniques—including spin coating, slot-die printing, inkjet printing, and photo-crosslinking—have further enabled large-area uniformity, precise thickness control, and contamination-free interfaces. These advances have translated into significant improvements in electrical and optoelectrical performance, including high carrier mobility, low-voltage operation, and high photoresponsivity. Moreover, recent demonstrations of reconfigurable operation modes highlight the potential of vdW thin films for advanced optoelectronic device applications, where a single device configuration can operate as both a high-speed photodetector and photosynapse devices.

Looking forward, the continued development of vdW thin films will further accelerate their integration into scalable electronic and optoelectronic platforms. Future research should focus on refining scalable processing techniques to achieve full back-end-of-line compatibility while maintaining uniformity and interface quality. In parallel, exploring new material combinations for heterogeneous stacking can enhance device performance, broaden operational wavelength ranges, and enable multifunctional operation. With these advancements, solution-processed vdW thin films are poised to serve as a versatile platform for high-performance, large-area electronic and optoelectronic systems, paving the way for practical, next-generation applications.

### CRediT Authorship Contribution Statement

**Jihyun Kim**: Conceptualization, Visualization, Writing – original draft. **Joohoon Kang**: Conceptualization, Project administration, Supervision, Writing – review & editing.

### Declaration of Competing Interest

All authors declare that they have no competing financial interests or personal relationships that may have influenced the work reported in this study.

### Acknowledgements

J. Kang acknowledges the research funds provided by the Ministry of Trade, Industry & Energy (RS-2024-00420534).

## REFERENCES

[1] Y. Liu, X. Duan, H.-J. Shin, S. Park, Y. Huang, X. Duan, Promises and prospects of two-dimensional transistors, Nature 591 (2021) 43–53.
[2] F. Koppens, T. Mueller, P. Avouris, A. Ferrari, M.S. Vitiello, M. Polini, Photodetectors based on graphene, other two-dimensional materials and hybrid systems, Nat. Nanotechnol. 9 (2014) 780–793.
[3] X. Huang, C. Liu, P. Zhou, 2D semiconductors for specific electronic applications: from device to system, npj 2D Mater. Appl. 6 (2022) 51.
[4] D. Akinwande, C. Huyghebaert, C.-H. Wang, M.I. Serna, S. Goossens, L.-J. Li, et al., Graphene and two-dimensional materials for silicon technology, Nature 573 (2019) 507–518.
[5] S. Wang, X. Liu, M. Xu, L. Liu, D. Yang, P. Zhou, Two-dimensional devices and integration towards the silicon lines, Nat. Mater. 21 (2022) 1225–1239.
[6] X. Hong, J. Kim, S.-F. Shi, Y. Zhang, C. Jin, Y. Sun, et al., Ultrafast charge transfer in atomically thin MoS2/WS2 heterostructures, Nat. Nanotechnol. 9 (2014) 682–686.
[7] A. K. Geim, I.V. Grigorieva, Van der Waals heterostructures, Nature 499 (2013) 419–425.
[8] A. Castellanos-Gomez, X. Duan, Z. Fei, H.R. Gutierrez, Y. Huang, X. Huang, et al., Van der Waals heterostructures, Nat. Rev. Methods Primers 2 (2022) 58.
[9] K.S. Novoselov, A. Mishchenko, A. Carvalho, A. Castro Neto, 2D materials and van der Waals heterostructures, Science 353 (2016) aac9439.
[10] Y. Liu, N.O. Weiss, X. Duan, H.-C. Cheng, Y. Huang, X. Duan, Van der Waals heterostructures and devices, Nat. Rev. Mater. 1 (2016) 16042.
[11] D. Jariwala, T.J. Marks, M.C. Hersam, Mixed-dimensional van der Waals heterostructures, Nat. Mater. 16 (2017) 170–181.
[12] J.C. Song, N.M. Gabor, Electron quantum metamaterials in van der Waals heterostructures, Nat. Nanotechnol. 13 (2018) 986–993.
[13] Y.S. Cho, S.Y. Jung, J. Kang, The role of two-dimensional materials in optical chemical sensing, J. Sens. Sci. Technol. 34 (2025) 324–341.
[14] G.B. Nam, H.W. Jang, Recent advances and challenges of two-dimensional MXene-based chemoresistive gas sensors, J. Sens. Sci. Technol. 34 (2025) 375–386.
[15] H.-D. Lee, S. Lee, MoS2-based ultra-low-power NH3 gas sensor with room-temperature operation, J. Sens. Sci. Technol. 34 (2025) 159–162.
[16] B. Zhao, Z. Zhang, J. Xu, D. Guo, T. Gu, G. He, et al., Gate-driven band modulation hyperdoping for high-performance p-type 2D semiconductor transistors, Science 388 (2025) 1183–1188.
[17] D. Lee, J.J. Lee, Y.S. Kim, Y.H. Kim, J.C. Kim, W. Huh, et al., Remote modulation doping in van der Waals heterostructure transistors, Nat. Electron. 4 (2021) 664–670.
[18] L. Wang, S. Papadopoulos, F. Iyikanat, J. Zhang, J. Huang, T. Taniguchi, et al., Exciton-assisted electron tunnelling in van der Waals heterostructures, Nat. Mater. 22 (2023)

1094–1099.
[19] X. Li, Z. Li, J. Hu, B. Huang, J. Shi, Z. Zhong, et al., Tunneling-barrier-controlled sensitive deep ultraviolet photodetectors based on van der Waals heterostructures, Nat. Commun. 16 (2025) 2209.
[20] J. Kim, O. Song, Y.S. Cho, M. Jung, D. Rhee, J. Kang, Revisiting solution-based processing of van der Waals layered materials for electronics, ACS Mater. Au 2 (2022) 382–393.
[21] T. Zou, Y.-Y. Noh, Solution-processed 2D transition metal dichalcogenides: materials to CMOS electronics, Acc. Mater. Res. 4 (2023) 548–559.
[22] O. Song, J. Kang, Solution-processed 2D materials for electronic applications, ACS Appl. Electron. Mater. 5 (2023) 1335–1346.
[23] S. Wang, W. Li, J. Xue, J. Ge, J. He, J. Hou, et al., A library of 2D electronic material inks synthesized by liquid-metal-assisted intercalation of crystal powders, Nat. Commun. 15 (2024) 6388.
[24] J.N. Coleman, M. Lotya, A. O'Neill, S.D. Bergin, P.J. King, U. Khan, et al., Two-dimensional nanosheets produced by liquid exfoliation of layered materials, Science 331 (2011) 568–571.
[25] J. Kim, S. Kim, Y.S. Cho, M. Choi, S.-H. Jung, J.H. Cho, et al., Solution-processed MoS2 film with functional interfaces via precursor-assisted chemical welding, ACS Appl. Mater. Interfaces 13 (2021) 12221–12229.
[26] J. Kang, J.-W. T. Seo, D. Alducin, A. Ponce, M.J. Yacaman, M.C. Hersam, Thickness sorting of two-dimensional transition metal dichalcogenides via copolymer-assisted density gradient ultracentrifugation, Nat. Commun. 5 (2014) 5478.
[27] J. Kang, J.D. Wood, S.A. Wells, J.-H. Lee, X. Liu, K.-S. Chen, et al., Solvent Solvent exfoliation of electronic-grade, two-dimensional black phosphorus, ACS Nano 9 (2015) 3596–3604.
[28] J. Kang, S.A. Wells, J.D. Wood, J.-H. Lee, X. Liu, C.R. Ryder, et al., Stable aqueous dispersions of optically and electronically active phosphorene, Proc. Natl. Acad. Sci. U.S.A. 113 (2016) 11688–11693.
[29] J. Kang, S.A. Wells, V.K. Sangwan, D. Lam, X. Liu, J. Luxa, et al., Solution-based processing of optoelectronically active indium selenide, Adv. Mater. 30 (2018) 1802990.
[30] Z. Lin, Y. Huang, X. Duan, Van der Waals thin-film electronics, Nat. Electron. 2 (2019) 378–388.
[31] D. Rhee, D. Jariwala, J.H. Cho, J. Kang, Solution Solution-processed 2D van der Waals networks: fabrication strategies, properties, and scalable device applications, Appl. Phys. Rev. 11 (2024) 021310.
[32] Z. Lin, Y. Liu, U. Halim, M. Ding, Y. Liu, Y. Wang, et al., Solution-processable 2D semiconductors for high-performance large-area electronics, Nature 562 (2018) 254–258.
[33] J. Kim, D. Rhee, O. Song, M. Kim, Y.H. Kwon, D.U. Lim, et al., All-solution-processed van der Waals heterostructures for wafer-scale electronics, Adv. Mater. 34 (2022) 2106110.
[34] J. Kim, D. Rhee, M. Jung, G.J. Cheon, K. Kim, J.H. Kim, et al., Defect-engineered semiconducting van der Waals thin film at metal–semiconductor interface of field-effect transistors, ACS Nano 18 (2024) 1073–1083.
[35] Y.A. Kwon, J. Kim, S.B. Jo, D.G. Roe, D. Rhee, Y. Song, et al., Wafer-scale transistor arrays fabricated using slot-die printing of molybdenum disulfide and sodium-embedded alumina, Nat. Electron. 6 (2023) 443–450.
[36] O. Song, D. Rhee, J. Kim, Y. Jeon, V. Mazánek, A. Söll, et al., All inkjet-printed electronics based on electrochemically exfoliated two-dimensional metal, semiconductor, and dielectric, npj 2D Mater. Appl. 6 (2022) 64.
[37] T. Carey, S. Cacovich, G. Divitini, J. Ren, A. Mansouri, J.M. Kim, et al., Fully inkjet-printed two-dimensional material field-effect heterojunctions for wearable and textile electronics, Nat. Commun. 8 (2017) 1202.
[38] G. Hu, L. Yang, Z. Yang, Y. Wang, X. Jin, J. Dai, et al., A general ink formulation of 2D crystals for wafer-scale inkjet printing, Sci. Adv. 6 (2020) eaba5029.
[39] I.C. Kwak, J. Kim, J.W. Moon, S. Kim, J.Y. Park, O. Song, et al., Orthogonal photopatterning of two-dimensional percolated network films for wafer-scale heterostructures, Nat. Electron. 8 (2025) 235–243.
[40] I.C. Kwak, S.J. Kim, W.H. Cho, J. Kim, S. Kim, Y.A. Kwon, et al., Direct photopatterning of green solvent-processed 2D nanomaterials for wafer-scale electronics, Adv. Mater. 37 (2025) e05917.
[41] K. Kim, J. Kim, M. Jung, I.S. Kim, B.-S. Yu, S.M. Won, et al., Sub-stoichiometric zirconium oxide as a solution-processed dielectric for reconfigurable electronics, Nat. Electron. 8 (2025) 461–473.
[42] M. Choi, Y.J. Park, B.K. Sharma, S.-R. Bae, S.Y. Kim, J.-H. Ahn, Flexible Flexible active-matrix organic light-emitting diode display enabled by MoS2 thin-film transistor, Sci. Adv. 4 (2018) eaas8721.
[43] Y.J. Park, B.K. Sharma, S.M. Shinde, M.-S. Kim, B. Jang, J.-H. Kim, et al., All MoS2-based large area, skin-attachable active-matrix tactile sensor, ACS Nano 13 (2019) 3023–3030.
[44] S. Ji, S.R. Bae, L. Hu, A.T. Hoang, M.J. Seol, J. Hong, et al., Perovskite light-emitting diode display based on MoS2 backplane thin-film transistors, Adv. Mater. 36 (2024) 2309531.
[45] M. Choi, S.-R. Bae, L. Hu, A.T. Hoang, S.Y. Kim, J.-H. Ahn, Full-color active-matrix organic light-emitting diode display on human skin based on a large-area MoS2 backplane, Sci. Adv. 6 (2020) eabb5898.
[46] A.T. Hoang, L. Hu, B.J. Kim, T.T.N. Van, K.D. Park, Y. Jeong, et al., Low Low-temperature growth of MoS2 on polymer and thin glass substrates for flexible electronics, Nat. Nanotechnol. 18 (2023) 1439–1447.
[47] Y. Jeon, D. Rhee, B. Wu, V. Mazanek, I.S. Kim, D. Son, et al., Electrochemically exfoliated phosphorene nanosheet thin films for wafer-scale near-infrared phototransistor array, npj 2D Mater. Appl. 6 (2022) 82.
[48] T. Hassan, J. Kim, H.N. Manh, A. Iqbal, Z. Gao, H. Kim, et al., Semiconducting properties of delaminated titanium nitride Ti4N3Tx MXene with gate-tunable electrical conductivity, ACS Nano 18 (2024) 23477–23488.
[49] D. Rhee, J. Kim, J. Kang, Solution-Processed Two-

Dimensional Materials for Scalable Production of Photodetector Arrays, J. Sens. Sci. Technol. 31 (2022) 228-237.
[50] O. Song, D. Rhee, J. Kim, M. Jung, S. Kim, I.S. Kim, et al., Solution-processed 2D transition metal dichalcogenide networks for scalable, flexible photosynaptic device arrays, IEEE J. Sel. Top. Quantum Electron. 30 (2024) 1–8.

**Jihyun Kim** is a postdoctoral researcher in the Department of Chemical and Biomolecular Engineering at Yonsei University. He received his Ph.D. degree in Advanced Materials Science & Engineering from Sungkyunkwan University under the supervision of Prof. Joohoon Kang. His research focuses on fabrication of solution-processed van der Waals thin films, and their applications for electronic and optoelectronic devices.

**Prof. Joohoon Kang** is an Associate Professor in the Department of Chemical and Biomolecular Engineering at Yonsei University. He received his B.S. and M.S. degrees in materials science and engineering from Yonsei University in Korea in 2009 and 2011, respectively, and his Ph.D. degree in materials science and engineering from Northwestern University in 2018. He then moved to the University of California at Berkeley as a postdoctoral fellow in the College of Chemistry. His research interests include synthesis, processing, and (opto)electronic applications of nanomaterials. For more information, please visit the website: http://mfmp.yonsei.ac.kr